

This copy is for your personal, non-commercial use only.

If you wish to distribute this article to others, you can order high-quality copies for your colleagues, clients, or customers by [clicking here](#).

Permission to republish or repurpose articles or portions of articles can be obtained by following the guidelines [here](#).

The following resources related to this article are available online at www.sciencemag.org (this information is current as of March 6, 2011):

Updated information and services, including high-resolution figures, can be found in the online version of this article at:

<http://www.sciencemag.org/content/331/6017/565.full.html>

Supporting Online Material can be found at:

<http://www.sciencemag.org/content/suppl/2011/02/01/331.6017.565.DC1.html>

A list of selected additional articles on the Science Web sites **related to this article** can be found at:

<http://www.sciencemag.org/content/331/6017/565.full.html#related>

This article **cites 16 articles**, 5 of which can be accessed free:

<http://www.sciencemag.org/content/331/6017/565.full.html#ref-list-1>

This article has been **cited by** 1 articles hosted by HighWire Press; see:

<http://www.sciencemag.org/content/331/6017/565.full.html#related-urls>

This article appears in the following **subject collections**:

Physics

<http://www.sciencemag.org/cgi/collection/physics>

17. A. Claret, A. Giménez, *Astron. Astrophys.* **277**, 487 (1993).
18. R. A. Brooker, T. W. Olle, *Mon. Not. R. Astron. Soc.* **115**, 101 (1955).
19. G. Torres, C. H. Lacy, L. A. Marschall, H. A. Sheets, J. A. Mader, *Astrophys. J.* **640**, 1018 (2006).
20. M. López-Morales, *Astrophys. J.* **660**, 732 (2007).
21. J. C. Morales, I. Ribas, C. Jordi, *Astron. Astrophys.* **478**, 507 (2008).
22. A. Kraus *et al.* (2010); preprint available at <http://arxiv.org/abs/1011.2757>.
23. I. Baraffe *et al.*, *Astron. Astrophys.* **337**, 403 (1998).
24. L. Siess, E. Dufour, M. Forestini, *Astron. Astrophys.* **358**, 593 (2000).
25. B.-O. Demory *et al.*, *Astron. Astrophys.* **505**, 205 (2009).
26. K. Vida *et al.*, *Astron. Astrophys.* **504**, 1021 (2009).
27. P. Demarque, J.-H. Woo, Y.-C. Kim, S. K. Yi, *Astrophys. J. Suppl. Ser.* **155**, 667 (2004).
28. Ö. Çakırlı, C. Ibanoglu, A. Dervisoglu, *Rev. Mex. Astron. Astrofis.* **46**, 363 (2010).
29. Funding for this Discovery mission is provided by NASA's Science Mission Directorate. J.A.C. and D.C.F. are Hubble Fellows and acknowledge support for this work by NASA through Hubble Fellowship grants HF-51267.01-A and HF-51272.01-A awarded by the Space Telescope Science Institute, which is operated by the Association of Universities for Research in Astronomy, Inc., for NASA under contract NAS 5-26555. J.A.C. is grateful for helpful

discussions with P. Podsiadlowski, S. Rappaport, G. Torres, A. Levine, J. Winn, S. Seager, and T. Dupuy. J.F.R. is a NASA Postdoctoral Program Fellow.

Supporting Online Material

www.sciencemag.org/cgi/content/full/science.1201274/DC1
Materials and Methods
Figs. S1 to S7
Table S1
Movie S1
References

6 December 2010; accepted 4 January 2011
Published online 11 January 2011;
10.1126/science.1201274

Ultralong-Range Polaron-Induced Quenching of Excitons in Isolated Conjugated Polymers

Joshua C. Bolinger,*† Matthew C. Traub,* Takuji Adachi, Paul F. Barbara

In conjugated polymers, radiative recombination of excitons (electron-hole pairs) competes with nonradiative thermal relaxation pathways. We visualized exciton quenching induced by hole polarons in single-polymer chains in a device geometry. The distance-scale for quenching was measured by means of a new subdiffraction, single-molecule technique—bias-modulated intensity centroid spectroscopy—which allowed the extraction of a mean centroid shift of 14 nanometers for highly ordered, single-polymer nanodomains. This shift requires energy transfer over distances an order of magnitude greater than previously reported for bulk conjugated polymers and far greater than predicted by the standard mechanism for exciton quenching, the unbiased diffusion of free excitons to quenching sites. Instead, multistep “energy funneling” to trapped, localized polarons is the probable mechanism for polaron-induced exciton quenching.

The performance of conjugated polymer (CP)-based electro-optic devices, such as light-emitting diodes and organic photovoltaic solar cells, can be degraded via quenching of the excitons (electron-hole pairs) through their interaction with hole polarons (p^+). Previous electrical and single-molecule spectroscopic experiments have demonstrated the existence of p^+ traps in CPs (1, 2). As in the more extensively studied quenching of electrically excited molecules by electron acceptors in dilute solution, exciton-quenching in the solid state is expected to occur through electron transfer from the exciton to p^+ . In conjugated polymers, the exciton-to-polaron electron transfer process results in spatial displacement and detrapping of the hole (3, 4). The limited spatial resolution of conventional far-field fluorescence microscopy has constrained the ability to make real-space measurements of the distance scale for exciton/polaron quenching (5). Instead, it has been investigated primarily by means of ensemble measurements of fluorescence quenching induced by charge injection from elec-

trodes on bulk samples (6). Such measurements, which are not spatially resolved and are indirect in nature, can be misleading because they spatially average over a highly disordered morphology. As a result, very little is known at the molecular level about the mechanism of polaron-induced exciton quenching.

We introduce an electro-optical, subdiffraction single-molecule spectroscopy imaging technique: bias-modulated intensity-centroid spectroscopy (BIC) (7). We used this method to spatially resolve the distance scale for fluorescence quenching caused by singlet exciton deactivation by p^+ in isolated single-polymer chains of poly[2-methoxy-5-(2'-ethyl-hexyloxy)-1,4-phenylene vinylene] (MEH-PPV) embedded in a non-conducting polymer, poly(methyl methacrylate) (PMMA). BIC combines single-molecule spectroscopic techniques that were previously introduced for the investigation of exciton/polaron interactions (1, 8) with subdiffraction single-molecule imaging methods, such as photoactivated localization microscopy (PALM) and stochastic optical reconstruction microscopy (STORM) (9–11), that allow for the localization of fluorescent dyes in biological samples on the <10-nm scale. In contrast to PALM and STORM, BIC is designed to measure the distance scale of an electro-optical physical process, not just the molecular location.

In this study, a semiconductor capacitor-like device structure (Fig. 1A) was used to controllably charge and discharge single-polymer molecules with one or more p^+ by modulating the bias across the device in the appropriate range (I). Holes are injected from an adjacent-hole transport layer in contact with the single molecules.

The degree of charging of a particular molecule is indirectly measured by recording the synchronously averaged integrated intensity of its fluorescence spot (I_{FI}) (Fig. 1B) as a function of the bias $E(V)$ across the device, which is modulated periodically in a square-wave (Fig. 1C). For the bias conditions in Fig. 1, the quenching is about 60% during the more positive portion of the bias cycle, which corresponds to the injection of approximately one p^+ for a MEH-PPV macromolecule with a molecular weight (M_w) of ~150,000, the material studied in Fig. 1 (I, δ). The fluorescence intensity centroid of the single-CP molecule can be determined by a two-dimensional (2D) Gaussian fitting procedure of the time-dependent fluorescence images. This centroid was displaced periodically in the sample (x, y) plane as the bias was modulated, and in turn, the fluorescence quenching was initiated because of the p^+ injection (Fig. 1D). The total bias-dependent centroid displacement was calculated from the orthogonal (X and Y) displacements in the laboratory frame.

It is unlikely that observed centroid displacements are caused by actual translocation of the CP molecule because the materials that comprise the device are rigid solids. Instead, we assigned the observed displacement in centroid position to selective quenching of some of the ~100 different chromophores that comprise the 150,000 M_w multichromophoric single-CP molecule. On the basis of previous nonspatially resolved spectroscopic measurements and modeling studies (12), each single molecule is expected to be in a collapsed, approximately cylindrical conformation with dimensions in the ~5- by 200-nm range. Thus, despite the undoubtedly complex local intramolecular intensity pattern of emitting sites the spatial substructure in each conjugated polymer is difficult to resolve directly because of the diffraction limit. Control experiments verified that the observed centroid displacements are not caused by potential artifacts, such as sloping back-

Center for Nano and Molecular Science and Technology, University of Texas, Austin, TX 78712, USA.

*These authors contributed equally to this work.

†To whom correspondence should be addressed. E-mail: jcb2873@mail.utexas.edu

ground profiles, detector artifacts, or inaccuracies in the use of fitting with a single 2D Gaussian function to determine the centroid position for a closely spaced collection of emitting chromophores (fig. S3).

A striking feature of the results in Fig. 1D is that the centroid displacements as a function of bias are nearly identical for each cycle. This pattern allows for synchronous averaging of the displacement data, leading to an improved signal-to-noise ratio for the X and Y components of the centroid determination with a mean SD for the X and Y position determination as small as 0.5 nm, despite a diffraction limit of ~ 300 nm (Fig. 1E). The plateaus in the X and Y component data in Fig. 1E for the vast majority of the molecules investigated ($>95\%$) exhibited roughly constant values during the uncharged (lower bias) and charged (higher bias) periods and reflected the X , Y centroid positions that correspond to these two cases. These data can be used to calculate the magnitude of the in-plane vector displacement, D , of the centroid induced by p^+ injection into the molecule. For the molecule portrayed in Fig. 1, C to E, this procedure gives a measured D value of 29.4 ± 3.9 nm.

A histogram of D values for 167 molecules of MEH-PPV (Fig. 1F) shows that the magnitudes of the displacements range from 0 to over 60 nm with a peak and mean displacement of 9.8 nm and 13.7 nm, respectively. The p^+ -induced quenching for the molecules in this histogram falls in the range of 40 to 80%, with a mean of about 60%. On the basis of previous photooxidation studies, for single-CP chains this quenching depth corresponds to ~ 1 charge per molecule (13). The reproducibility of D (and its X and Y components) over repeated charging cycles implies energy transfer from excited chromophores to a single stationary (or trapped) p^+ , which is injected to the same location along the polymer chain for all cycles for a given molecule. This is strong evidence for the previous proposal that a p^+ injected into a single-polymer chain located on an organic electrode is trapped in a pre-existing site with a low-energy highest occupied molecule orbital (HOMO) (I). One candidate for a low-HOMO-energy site for p^+ is a location along the polymer chain where the chain makes extraordinarily close contact with itself, allowing for π -stacking interactions that can stabilize the hole through delocalization ($I4$).

The dynamics of this displacement of the intensity centroid caused by trapped p^+ can be explored by considering simulations of the quenching of a multichromophoric molecule. Because charge transfer processes are most effective at distances of <1 nm, we hypothesize that the actual charge transfer–quenching step is preceded by multiple Förster energy transfer events, each of which can operate at distances of ~ 5 nm. Presented in Fig. 2A is a graphical representation of a polymer chain embedded in the charge injection device. The chain was generated by means of a previously described beads-on-a-chain Monte Carlo simulation that is capable of producing

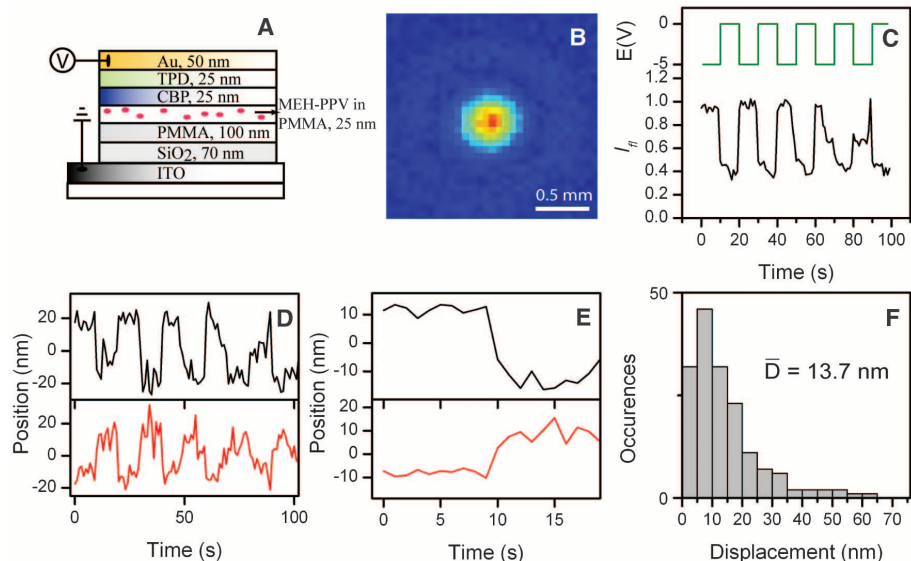
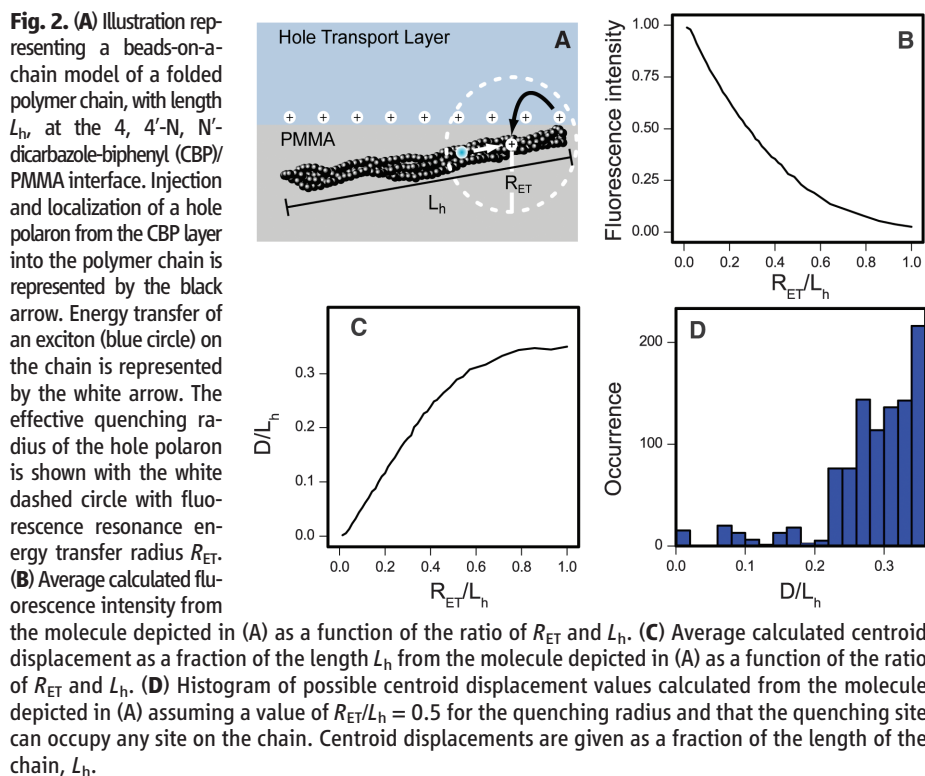


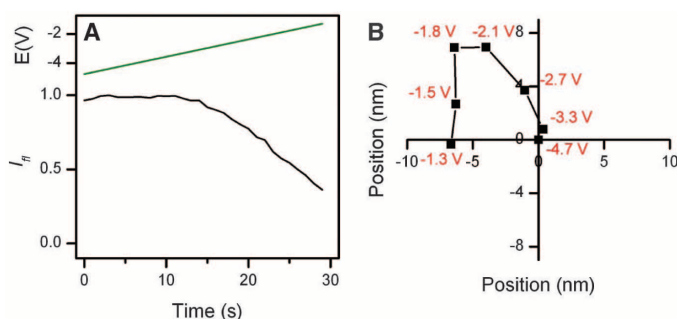
Fig. 1. (A) Structure of the hole-injection device used in these studies. (B) False-color image of a single molecule of MEH-PPV imbedded in the hole-only device. (C) Fluorescence-voltage (F - V) measurement of the molecule shown in (B), in which the fluorescence trajectory is shown in black and the applied bias is shown above, in green. (D) The centroid displacement of the fluorescence point spread function resulting from the applied bias shown in (C), in which displacement in the x direction is shown at top (black), and y is shown at bottom (red). (E) Synchronized average of the X (black line) and Y (red line) centroid displacement obtained from (D). (F) Histogram of the total centroid displacement ($D = \sqrt{X^2 + Y^2}$) for 167 different single-molecule MEH-PPV ($M_w = 150,000$) transients. Values peak at 9.8 nm, whereas the mean value is 13.7 nm.



many different molecular configurations ($I2$). The exact conformation of a single-polymer molecule is unknown; however, given the extraordinary distances over which centroid displacement is

occurring one molecular axis must be relatively large compared with the others. In support of this hypothesis, lattice models with a fixed volume were constructed in order to simulate multichromophore

Fig. 3. (A) Synchronously averaged fluorescence transient of a single molecule (black), with the ramp bias applied as shown above (green). **(B)** Synchronized average of the point spread function centroid position obtained from the single molecule shown in (A), with the voltage for each point shown in red (some points omitted for clarity).



molecule quenching via a Förster-type process. The results of these simulations (fig. S2) suggest that only highly asymmetric configurations (a long, rectangular lattice array as opposed to a cubic one) can produce large centroid displacements. Additionally, current work on absorption polarization of single-polymer chains of MEH-PPV demonstrates a single population of molecular conformations with a high anisotropy value (15). Coupled with the large centroid displacements observed in this work, we propose that a needle-like structure as shown in Fig. 2A is appropriate.

Using the molecular conformation shown in Fig. 2A, a simulation similar to the lattice model was performed in which each bead is an individual chromophore. A random bead on the chain was assigned as a quenching site. For illustrative purposes, we used a single-step Förster quenching mechanism as described in (7) and varied the distance of energy transfer (R_{ET}) relative to the length of the molecule (L_h). The impact of changing this distance on the centroid displacement is presented in Fig. 2, B to D. Simulated average fluorescence intensity as a function of the ratio of R_{ET} and L_h is shown in Fig. 2B. Unsurprisingly, values of R_{ET}/L_h of 0 and 1 produce no fluorescence quenching and complete fluorescence quenching, respectively, whereas $R_{ET}/L_h = 0.5$ produces 75% fluorescence quenching.

Average centroid displacement versus energy transfer distance is compared in Fig. 2C. The centroid displacement plateaus at a value of $\sim 1/3$ the length of the molecular axis at high values of R_{ET} . Figure 2D plots the distribution of centroid displacements calculated for $R_{ET}/L_h = 0.5$, and with this parameter, the displacements are weighted heavily between 25 and 35% of the length of the folded polymer chain. The large D values (such as >10 nm) thus imply that one molecular axis of the polymer chain must be at least three times the size of the observed displacement and are only observed for R_{ET} values that are >25 nm and in some cases >75 nm.

These R_{ET} values are much greater than the largest R_{ET} values calculated for Förster energy transfer between two well-aligned CP chromophores with excellent spectral overlap ($R_{ET} < 6$ nm). Unsurprisingly, preceding the exciton quenching with a single-step, downhill energy transfer by a Förster mechanism is inconsistent with the observed centroid displacement results. Instead, it is

probable that multistep interchromophore energy transfer precedes the actual quenching step. The bulk diffusion length of 5 nm (6) for energy migration in PPVs is, however, too small to explain the up-to-60-nm observed exciton-quenching lengths. It may be that energy diffusion is more rapid and occurs over a larger distance for single-polymer chains than for bulk CP materials. BIC measurements of aggregated nanoparticles of MEH-PPV confirm this, showing an order of magnitude smaller centroid displacement upon charge injection (fig. S1). Single-polymer chains are more ordered than chains in the bulk materials, and are more favorable for rapid energy diffusion. Furthermore, single-polymer chains contain few if any “red” sites (low energy-emitting sites), which are known to effectively trap excitons in bulk materials (16).

Previous studies have modeled exciton relaxation in single conjugated polymer chains, suggesting that disorder in the chain prevents long-distance energy transfer (17). Directional energy transfer (energy funneling) in an ordered system toward the trapped polaron would be especially effective at producing large centroid displacements in the BIC experiment because it achieves a large displacement with a small number of hops. Energy funneling could be enhanced by a spatially dependent Stark effect on the S_1 - S_0 energy gaps of the chromophores in the vicinity of p^+ . This process would enhance both the rate and degree of directionality of the energy transfer process. Another hypothetical mechanism for enhanced energy funneling is an ultralong-range electron transfer involving rare delocalized electronic states (18).

The single-molecule D measurements reported in Fig. 1 correspond to quenching depths of $\sim 60\%$, which for 150,000 M_w molecules corresponds to roughly one p^+ . In order to explore the interaction of more than one p^+ , we recorded D values for larger quenching depths. We used a bias waveform with a repetitive linear ramp function rather than the square wave used for the experiments in Fig. 1. The X and Y components of the displacement are plotted in Fig. 3B for various times on the synchronously averaged data. The biases that correspond to each time are written in red next to each X, Y pair, and a line is drawn through the data to guide the eye. From -3.3 to -2.1 V, the apparent X, Y displacements increase

in magnitude because of an increase in the fraction of the time the molecule is occupied by a p^+ . Throughout this bias range, the best-fit D value increases, whereas the in-plane direction of displacement is unchanged. As the bias is varied to be even less negative, the Y displacement abruptly reverses. This reversal is assigned to quenching from a second and perhaps third charge in the molecule, which becomes a larger factor in the displacement data for the least negative biases. This experiment was reproduced for 50 molecules, and an analogous effect was observed (fig. S4). These data suggest that the position of the second injected p^+ is not colocalized with the injected hole but rather at a remote location. These results represent spatially resolved evidence against the bipolaron hypothesis—that the p^+ are not coupled. Instead, the location (perhaps random) of the trapped p^+ species is probably dictated by the location of low-energy sites in the polymer chain conformation.

References and Notes

- J. C. Bolinger, L. Fradkin, K. J. Lee, R. E. Palacios, P. F. Barbara, *Proc. Natl. Acad. Sci. U.S.A.* **106**, 1342 (2009).
- S. H. Lim, T. G. Bjorklund, C. J. Bardeen, *J. Chem. Phys.* **118**, 4297 (2003).
- J. Bolinger, K. J. Lee, R. E. Palacios, P. F. Barbara, *J. Phys. Chem. C* **112**, 18608 (2008).
- A. Salileo, R. A. Street, *J. Appl. Phys.* **94**, 471 (2003).
- D. M. Adams, J. Kerimo, D. B. O'Connor, P. F. Barbara, *J. Phys. Chem. A* **103**, 10138 (1999).
- D. E. Markov, E. Amsterdam, P. W. M. Blom, A. B. Sieval, J. C. Hummelen, *J. Phys. Chem. A* **109**, 5266 (2005).
- Materials and methods are available as supporting material on Science Online.
- P. F. Barbara, A. J. Gesquiere, S. J. Park, Y. J. Lee, *Acc. Chem. Res.* **38**, 602 (2005).
- E. Betzig *et al.*, *Science* **313**, 1642 (2006).
- W. E. Moerner, *Proc. Natl. Acad. Sci. U.S.A.* **104**, 12596 (2007).
- M. J. Rust, M. Bates, X. W. Zhuang, *Nat. Methods* **3**, 793 (2006).
- D. H. Hu *et al.*, *Nature* **405**, 1030 (2000).
- J. Yu, N. W. Song, J. D. McNeill, P. F. Barbara, *Isr. J. Chem.* **44**, 127 (2004).
- J. Yu, D. H. Hu, P. F. Barbara, *Science* **289**, 1327 (2000).
- T. Adachi *et al.*, *J. Phys. Chem. C*, **114**, 20896 (2010).
- D. Y. Kim, J. K. Grey, P. F. Barbara, *Synth. Met.* **156**, 2, 336 (2006).
- T. E. Dykstra *et al.*, *J. Phys. Chem. B* **113**, 656 (2009).
- E. Collini, G. D. Scholes, *Science* **323**, 369 (2009).
- We acknowledge funding by the U.S. Department of Energy Basic Energy Sciences, Solar Photochemistry Program, and the Welch Foundation. Before his death in October 2010, Dr. Barbara was the director of the Center for Nano and Molecular Science and Technology at the University of Texas, Austin, TX 78712. J.C.B. was a research scientist for Dr. Barbara at the time. Submission of this manuscript was done by J.C.B. subsequent to Dr. Barbara's death.

Supporting Online Material

www.sciencemag.org/cgi/content/full/331/6017/565/DC1
Materials and Methods
Figs. S1 to S4
References

15 October 2010; accepted 10 December 2010
10.1126/science.1199140